Numerical Analysis of Shear-off Failure of Keyed Epoxied Joints in Precast Concrete Segmental Bridges

Rabee Shamass[1]; Xiangming Zhou, Ph.D., M.ASCE[2]; Zongyi Wu[3]

[1]PhD Student in Civil Engineering, College of Engineering, Design and Physical Sciences, Brunel University London, Kingston Lane, Uxbridge, Middlesex UB8 3PH, United Kingdom Email: Rabee.Shamass@brunel.ac.uk

[2]Reader in Civil Engineering Design, College of Engineering, Design and Physical Sciences, Brunel University London, Kingston Lane, Uxbridge, Middlesex UB8 3PH, United Kingdom, Tel: +44 1895 266 670, Fax: +44 1895 256 392, Email: Xiangming.Zhou@brunel.ac.uk

[3]MSc in Structural Engineering, College of Engineering, Design and Physical Sciences, Brunel University London, Kingston Lane, Uxbridge, Middlesex UB8 3PH, United Kingdom, Email: bs14zzw@my.brunel.ac.uk

Abstract: Precast concrete segmental box girder bridges (PCSBs) are becoming increasingly popular in modern bridge construction. The joints in PCSBs are of critical importance which largely affects the overall structural behaviour of PCSBs. The current practice is to use unreinforced small epoxied keys distributed across the flanges and webs of a box girder cross section forming a joint. In this paper, finite element analysis was conducted to simulate the shear behaviour of unreinforced epoxied joints, which are the single-keyed and three-keyed to represent multiple-keyed epoxied joints. The concrete damaged plasticity model along with the pseudo-damping scheme were incorporated to analyse the key assembly for microcracks in the concrete material and to stabilize the solution, respectively. In numerical analyses, two values of concrete tensile strength were adapted, the one from Eurocode 2 formula and the one of general assumption of tensile strength of concrete, 10%f_{cm}. The epoxy was modelled as linear elastic material since the tensile and shear strength of the epoxy were much higher than those of the concrete. The numerical model was calibrated by full-scale experimental results from literature. Moreover, it was found that the numerical results of the joints, such as ultimate shear load and crack initiation and propagation, agreed well with experimental results. Therefore, the numerical model associated with relevant parameters developed in this study was validated. The numerical model was then used for parametric study on factors affecting shear behaviour of keyed epoxied joints which are concrete tensile strength, elastic modulus of epoxy and confining pressure. It has been found that the tensile strength of concrete has significant effect on the shear capacity of the joint and the displacement at the ultimate load. A linear relationship between the confining pressure and the shear strength of single-keyed epoxied joints was observed. Moreover, the variation in elastic modulus of epoxy does not affect the ultimate shear strength of the epoxied joints when it is greater than 25% of elastic modulus of concrete. Finally, an empirical formula published elsewhere for assessing the shear strength of single-keyed epoxied joints was modified based on the findings of this research to be an explicit function of tensile strength of concrete.

CE Database subject headings: Concrete bridges; Failure modes; Finite element method; Girder bridge; Joints; Precast concrete; Shear; Shear failures; Shear strength

Author Keywords: Concrete damage plasticity; Direct shear; Empirical formula; Epoxied joint; Keyed joints; Precast concrete segmental bridges; Shear-off

Introduction

With the advancement of the design and construction technologies, precast concrete segmental box girder bridges (PCSBs) has become increasingly popular in modern bridge construction. PCSBs have excellent durability and low life-cycle cost, solving a range of problems in bridge design, construction and maintenance. The joints between the precast segments are of critical importance in segmental bridge construction. They are critical to the development of structural capacity and integrity by ensuring the transfer of shear across the joints and often play a key role in ensuring durability by protecting the tendons against corrosion (Koseki and Breen 1983). In other words, the serviceability and shear behaviours of PCSBs depend on the behaviour of the joints. Therefore, the performance of the joints affects the safety of a PCSB to a large degree. Reasonable design, ease of construction and high quality of the joints should be controlled strictly. Both epoxied joints and dry joints can be used in construction. However, epoxy is temperature sensitive and its performance would be affected by weather conditions, which consequently largely affects construction in the field when epoxied joints are used for PCSBs. Therefore, dry joints owing to simplicity in construction become more popular. However, AASHTO (2003) has prohibited the usage of dry joints due to potential durability problem. In this case, only epoxied joints are allowed in PCSBs. Usually, the thickness of epoxy is 1 mm and 2 mm. The keyed joints can be single-keyed or multiple-keyed. Experimental results of the keyed joints indicate that multi-keyed joints can resist higher shear load than single-keyed ones (Zhou et al. 2005; Alcalde et al. 2013). Also, the shear resistance of the keyed joints is significantly greater than that of the flat joints and joints with epoxy layer have higher shear resistance capacity and better durability than those without an epoxy layer, i.e. dry joints.

There are some experimental studies on epoxied shear keys reported by Buyukozturk et al. 1990; Zhou et al. 2005. The experiments by Zhou et al. (2005) present shear behaviours including normalised shear stress-displacement curves, cracking propagations and ultimate shear load of a range of single and multiple-keyed joints. A total 37 specimens were tested with different parameters by varying confining pressure, key number and interaction way between the male and female parts containing epoxy layer or dry contacting. Comparing the results from single- and multiple-keyed dry specimens, they showed similar crack behaviour initially, i.e. a 45 degree crack to the horizontal direction initiated at the bottom of the key and propagated upwards. At the same time, some small crack formed at the top of the male part as well. At the peak load, the cracks joined along the root of the male part and divided the male part to some extent; therefore, brittle slip occurred between the two concrete parts. On the other hand, brittle manner is the basic failure mode of epoxied joints. They suffer shear failure leading to brittle split between the male and female parts of the keyed joints. Crack propagation of single-keyed epoxied joints exhibits similar behaviour as flat epoxied joints. Initially, the crack formed at the bottom of the key and propagated along the shear plane at the ultimate load. At the same time, the crack formed at the top corner of the key and propagated with the increasing shear load. On the other hand, three-keyed epoxied joints exhibit a higher ductility due to longer cracking process than single-keyed epoxied joints. Buyukozturk et al. (1990) mainly compared the shear behaviour between dry and epoxied joints. From their experimental results, they observed that dry joints fail at a lower ultimate load than epoxied joints. On the other hand, dry joints process a higher ductility than the epoxied ones. Moreover, the adhesive strength of epoxy is nearly equal to, if not greater than, the concrete shear strength as judged from the failure mode of epoxied joints.

On the other hand, there are very limited numerical analyses on shear behaviour of keyed joints published. Rombach (1997) conducted numerical studies on keyed dry joints using ANSYS finite element code. Turmo et al. (2006) conducted FE study on the structural behaviour of simply supported segmental concrete bridges with dry and post-tension joints in which castellated keyed joints were analysed only using a flat joint model in order to avoid the fine mesh required for the keys in the full finite element model and therefore, reduce the computing time and cost. Similar techniques were employed by Kim et al. (2007) to study numerically a flat joint between precast post-tensioned concrete segments. Alcalde et al. (2013) developed a FE model of four different types of joints, with a number of keys varying between one and seven, to analyse the fracture behaviour of keyed dry joints under shear, focusing on the influence of the number of keys on the joint shear capacity and its average shear stress. Jiang et al. (2015) developed a finite-element model for dry keyed joints and verified the observed phenomenon of sequential failure of multi-keyed dry joints from the inferior key to the superior ones. Moreover, the numerical model of single-keyed dry joint which researched by Shamass et al. (2015) was calibrated and validated by Zhou et al. (2005) and Buyukozturk et al. (1990) experimental results. The differences in ultimate shear strength from numerical simulation and experiments are only in range of 9%, which indicates it was an effective model to simulate dry joint behaviour in PCSBs.

It can be seen that there are no numerical studies published on structural behaviour of keyed epoxied joints between concrete segments. In this paper, ABAQUS regards as a numerical tool to simulate the behaviour of single- and multi-keyed epoxied joints under confining pressure and monotonically increasing shear load. Moreover, the work provides data which are used to compare with the experimental results conducted by Zhou et al. (2005) and those by Buyukozturk et al. (1990), aiming to verify the numerical model. Data compared include ultimate shear strength and crack evolution in keyed zone for various joints. Using analysed numerical data, to compare with the experimental studies to propose more reliable, safe, serviceable and economical instructions of design of keyed epoxied joints. The numerical model was then employed for parametric studies on key parameters affecting structural behaviour of keyed epoxied joints which are the tensile strength of the concrete, Young's modulus of the epoxy and the confining pressures.

Numerical Model

Concrete Damage Plasticity Model

The concrete damaged plasticity (CDP) model is employed for modelling concrete. It assumes that the main two failure mechanisms of concrete are tensile cracking and compressive crushing (Simulia 2011). The CDP model is provided by ABAQUS code to present the plastic behaviour of concrete in both compressive and tensile conditions, namely, cracking under tension and crushing under compression. The CDP model can be used in application in which concrete subjected to either static loading or cyclic loading. The dilation angle, flow potential eccentricity, and viscosity parameter of the CDP model were assigned equal to 36, 0.1, and 0, respectively; the ratio of the strength in the biaxial state to the strength in the uniaxial state of concrete, f_{b0}/f_{c0} =1.16; and the ratio of the second stress invariant on the tensile meridian, K=0.667 (Kmiecik and Kaminski 2011).

Stress-Strain Curves of Concrete under Axial Compression

According to the Eurocode 2 (BSI 2004) which provides relationship of stress-strain in compression of concrete, the following expression is quoted:

$$\sigma_c = \left(\frac{k\,\eta - \eta^2}{1 + (k-2)\eta}\right) f_{cm} \tag{1}$$

Where:

$$\eta = \frac{\varepsilon_c}{\varepsilon_{c1}} \qquad k = 1.05\, E_{cm} \frac{\varepsilon_{c1}}{f_{cm}} \qquad \varepsilon_{c1}(‰) = 0.7(f_{cm})^{0.31} \leq 2.8 \qquad E_{cm} = 22(0.1\, f_{cm})^{0.3}$$

where E_{cm} is elastic modulus (in MPa) of concrete; and f_{cm} is ultimate compressive strength of concrete (in MPa). The strain at peak stress is ε_{c1}, and ultimate strain is ε_{cu1}, which is taken as 0.0035 according to Eurocode 2. Hooke's law presents a linear stress-strain relationship, which predicted up to 40% of ultimate compressive strength in the ascending branch. Inelastic strains $\tilde{\varepsilon}_c^{in}$ corresponding to compressive stresses σ_c were used in the CDP model. Additionally, the compressive damage parameter d_c needs to be defined at each inelastic strain level. It ranges from 0 for an undamaged material to 1 when the material has totally lost its loadbearing capacity. The value d_c is obtained only for the descending branch of the stress-strain curve of concrete in compression (see Shamass et al. (2015) on how to obtain $\tilde{\varepsilon}_c^{in}$ and d_c).

Tension softening

The tensile strength of concrete has a significant effect on the behaviour of the joint keys, as will be shown later. Therefore, two values of tensile strength have been used in the analysis. The first one is based on the Eurocode 2 (BSI 2004) with tensile strength in MPa given by

$$f_t = 0.3\,(f_{cm}-8)^{2/3} \tag{2}$$

The second one follows the general assumption, in which tensile strength is equal to 10% of the compressive strength of concrete. It is deserved to be noticed that the tensile strength suggested by Eurocode 2 is about 7%-7.5% of the compressive strength of the concretes tested by Buyukozturk et al. (1990) and Zhou et al. (2005).

Tension softening refers to the phenomenon that concrete can carry tension even after cracking, though tensile strength gradually decreases with increasing tensile strain. For structural elements where there is no or slight reinforcement in concrete, the approach based on the stress-strain relationship may introduce unreasonable mesh sensitivity to the results (Simulia 2011). Therefore, it is better to define the fracture energy or defining the stress-crack opening displacement curves. The softening behaviour of concrete can be defined using linear, bilinear and exponential expressions. The more accurate and realistic model is the exponential function which was experimentally derived by Cornelissen et al. (1986) and is adapted for this study:

$$\frac{\sigma_t}{f_t} = \left[1 - \left(c_1 \frac{w_t}{w_c}\right)^3\right] \exp\left(-\frac{c_2 w_t}{w_c}\right) - \frac{w_t}{w_c}(1 + c_1^3) \exp(-c_2) \qquad (3)$$

where σ_t is the concrete tensile stress, $c_1 = 3.0$ and $c_2 = 6.93$ are empirical constants, w_t is the crack opening displacement and $w_c = 5.14 G_f/f_t$ is the cracking displacement at the complete release of stress. The fracture energy G_f can be estimated following (Qureshi et al. 2011):

$$G_f = G_{f_0} \left(\frac{f_{cm}}{f_{cmo}}\right)^{0.7} \qquad (4)$$

where G_{f_0} is the base value of the fracture energy, which depends on the maximum aggregate size and is taken as 0.03 N/mm, and $f_{cmo} = 10\ \mathrm{MPa}$ is the base value of the mean compressive cylinder strength of concrete. Similarly to the case of compression, the tensile damage parameter d_t needs to be defined at each crack opening (see Shamass et al. (2015) on how to obtain d_t).

Crack Detection in Numerical Analysis

Due to the reason that the concrete damaged plasticity (CDP) model does not support the concept of cracking developing at the material integration point, the crack limitation recommended by Lubliner et al. (1989) is adopted in the current study. It assumed that cracking initiates at points where the tensile equivalent plastic strain is greater than zero and the maximum principle plastic strain is positive. The direction of the cracks is assumed to be orthogonal to the direction of maximum principle plastic stain at the damaged point.

Material Properties for Epoxy

Two types of epoxy were used by Buyukozturk et al. (1990) during their experiment, Dual 100 Type II and Ciba-Geigy Type HV. They claimed that there was no significant strength difference between the two types found in testing epoxied flat joints and the compressive strength of both epoxy was almost identical. The only mechanical properties available for the epoxy used from Bakhoum (1990), which Buyukozturk et al. (1990) was extracted from, are shown in the Table 1. Mays and Hutchinson (1992) reported that the typical value of tensile strength and shear strength of epoxy used in construction are 25 and 30 MPa, respectively. Buyukozturk et al. (1990) observed that the cracks propagated in the key's area through the shear plane of the male key and the concrete layer adjacent to the epoxy layer rather than the epoxy or the interface between the concrete and the epoxy.

Moreover, the bond strength of the concrete-epoxy interface is 22 MPa as shown in Table 1 as per Bakhoum (1990) which is much higher than the tensile strength of concrete. Therefore, the failure occurs due to the cracking in concrete and not at the concrete-epoxy interface. Moreover, the compressive strength of the epoxy is much higher than that of the concrete tested by Zhou et al. (2005) and Buyukozturk et al. (1990). Therefore the concrete crushes before the epoxy material fails in compression. The same argument applies for tensile strength in which the typical value of tensile strength of epoxy is much higher than that of the concretes tested by Zhou et al. (2005) and Buyukozturk et al. (1990). These experimental observations justify modelling the epoxy as elastic material and modelling concrete-epoxy interface as a perfect bond. These numerical assumptions will be checked later by numerical experiment. The same observations were found by Zhou et al. (2005) where the epoxy they used was Lanko 532 Utarep H80C made in France (Zhou et al. 2003). However, no information about the material properties of the used epoxy was provided. Therefore, the same material properties presented in Table 1 are used in the current numerical analysis.

Numerical Simulation

In this study, the single-keyed and multi-keyed epoxied joints tested by Zhou et al. (2005) and single-keyed epoxied joints tested by Buyukozturk et al. (1990) were analysed using FE code ABAQUS, version 6.11-1, based on the model parameters discussed above. In Zhou's specimens, the overall dimensions of the single-keyed epoxied joints were 500×620×250 mm^3 with 200×250 mm^2 the keyed area and 250 mm the thickness of the joint. The dimensions of the multi-keyed joints were 900×925×250mm^3 with 500×250 mm^2 the keyed area and 250 mm the thickness of the joint. The detailed dimensions of the joint and castellated keyed area are found in Zhou et al. (2005). The mesh size used in the numerical analysis was 4mm in the keyed area. 4-node bilinear plane stress quadrilateral elements (CPS4) were used for modelling the key assembly including the epoxy. The plane stress thickness was taken 250 mm. A full integration algorithm was used in numerical analyses. For these keyed joints tested by Zhou et al. (2005), the specimen identifier was represented as Mi-Ej-Kn, where i is the confining pressure in MPa, j is the epoxy thickness in mm and n is number of keys (1 or 3 keys). In the experiment reported by Buyukozturk et al. (1990), the overall dimensions of the single-keyed epoxied joints were 533.4×251×76.2 mm^3 with 154×76.2 mm^2 the keyed area and 76.2 mm the thickness of the joint. The detailed dimensions of the joint and castellated key are found in Buyukozturk et al. (1990) and the mesh size used in the numerical analysis was 3.5 mm. Similarly, 4-node bilinear plane stress quadrilateral elements (CPS4) with full integration algorithm were used and the plane stress thickness was taken 76.2 mm. A mesh-convergence analysis performed showed negligible changes in results by employing more refined meshes than those used to produce the presented results. Hence, it is concluded that there seems to be no particular issue with the accuracy of the FE modelling used here. An elastic perfectly-plastic model was used to simulate the material behaviour of reinforcement bar. The elastic modulus E_s, Poisson's ratio v and yield strength of steel were taken as 210 GPa, 0.30 and 400 MPa, respectively (see Zhou et al. (2005) and Buyukozturk et al. (1990) for reinforcement details and positions). In all cases, first-order truss elements were used for modelling the reinforcement bars embedded in the concrete keyed joints.

Simulation of Support and Applied Load

The whole joint assembly was subjected to static loading through a displacement-controlled loading from the loading head at the top surface of the joint. Displacement-controlled loading was simulated by boundary condition assigned to the loading head and moving downward. In order to model the experimental details at the top surface of Zhou's joints, a steel plate and rod steel were perfectly bonded to the top surface of the concrete by white cement mortar while a friction contact with friction coefficient equal to 0.78 (Gorst et al. 2003) was adapted between the streel rod and steel loading head (Figs. 1a & 1c). The width of the top steel plate was taken 62.5 mm as per real dimension in experiment. For the case of Buyukozturk's experiments, the contact between the steel loading head and the concrete was taken also as a friction contact with friction coefficient equal to 0.4 (ACI 1997).

The numerical model was controlled by two static-general steps assuming no large displacements happened in both steps. Moreover, in the displacement-controlled loading step, a specific dissipation energy fraction was selected for automatic stabilization with default value equals to 0.0002 in ABAQUS to avoid convergence difficulties due to local instabilities and to track the response after reaching the peak load. The confining pressure was simulated by load-mechanical-pressure on the side face of the joint which covers the keyed area (Fig. 1). The confining stress value is 1.0, 2.0, 3.0 MPa, respectively, covering the single-keyed area of 200×250 mm^2 and 0.5, 1.0, 1.5, 2.0 MPa covering the multi-keyed area of 500×250 mm^2, as per Zhou et al. (2005). Similarly, for the case of Buyukozturk et al. (1990) specimens, the confining pressure was applied covering keyed area of 154×76.2 mm^2 and assigned to general-static step. The confining pressure values were 0.69, 2.07 and 3.45 MPa, respectively, as per Buyukozturk et al. (1990). As the bottom surface contacts the ground, it has restrained against all transitional degree of freedom (Fig. 1).

The numerical analyses of multiple-keyed joints show that cracks in the concrete occur at the top of the joints and do not occur at the keyed area. This was confirmed experimentally by Zhou (Xiangming Zhou, personal communication, 16 December 2015), who used FRP to strengthen the top of the multiple-keyed epoxied joints to avoid such pre-failure then redid the test. That time the failure happened in the keyed area as desirable. To avoid such a problem in the numerical analysis, different numerical treatments were tried. Firstly, the reinforcement at the top of the joint was increased. This approach failed to avoid the failure of the key at the top since shear-off failure occurred at the area directly under the loading plate. Secondly, it was thought to model FRP to strengthen the top of the joint. However, this cannot be achieved in the current numerical analysis because the model is assumed to be in the state of 2D plane stress. Finally, the tensile strength of the concrete under the loading plate, i.e. the area away from the keyed area, was increased deliberately (about 5 times the normal value of tensile strength of concrete) (Fig. 1) for multiple-keyed epoxied joints. By such numerical treatment, the failure of the multiple-keyed joints happened at the keyed area as desirable.

FEA results

Ultimate shear strength of keyed epoxied joints

- ***For single-keyed epoxied joints***

The numerical analysis results, adapting Eurocode 2 and the general assumption of concrete tensile strength, of ultimate shear resistance capacity of epoxied joints are presented in Table 2. The numerical results are presented together with their counterpart experimental ones by Zhou et al. (2005) and Buyukozturk et al. (1990). Obviously, the ultimate shear strength of specimens with different concrete tensile strength is different. For Zhou's specimens and by using general assumption of concrete tensile strength (i.e. $f_t = 10\% f_{cm}$), the numerical analyses overestimate the shear strength for most of the specimens and the average absolute deviation from the experimental results is 18.0%. While using the concrete tensile strength calculated by Eurocode 2 formula, the absolute average deviation from the experimental results is 9.7%, i.e. in this case the numerical results (i.e. ultimate shear strength) generally are more conservative. The calculated ultimate loads in conjunction with the general assumption of tensile strength of concrete are in better agreement with experimental results for the specimens M2-E1-K1, M3-E1-K1, M2-E2-K1 and M3-E2-K1. The calculated ultimate loads in conjunction with the tensile strength of concrete calculated by Eurocode 2 formula are in better agreement with experimental results for the specimens M1-E1-K1, M1-E2-K1, M1-E3-K1, M2-E3-K1 and M3-E3-K1. Moreover, it can be noticed from Table 2 that the use of Eurocode 2 tensile strength in the numerical analyses reduces the predicted ultimate loads by about 12%-19% compared to those calculated based on the general assumption of tensile strength of concrete.

For Buyukozturk’s specimens and by use of concrete tensile strength calculated by Eurocode 2 formula, the numerical analyses underestimate the ultimate shear strength for all specimens compared with experiment, while the numerical ultimate loads calculated using general assumption of concrete tensile strength are all in better agreement with experimental one for all specimens. From Table 2, it can be noticed that the use of Eurocode 2 concrete tensile strength formula in the numerical analyses reduces the calculated ultimate loads by about 10%-22% compared to those obtained based on the general assumption of tensile strength of concrete, i.e. tensile strength of concrete is equal to 10% of its compressive strength.

The above examples show that the shear strengths of single-keyed epoxied joints are very sensitive to the value of concrete tensile strength. Additionally, adapting the concrete tensile strength by Eurocode 2 formula in the numerical simulation for the case of Zhou’s specimens and the general assumption of concrete tensile strength for the case of Buyukozturk’s specimens can provide shear strength of the joints generally in better agreement with the experimental ones, which will be used in the following sections.

- ***For multiple-keyed epoxied joints***

The numerical results of ultimate shear strength, adapting Eurocode 2 tensile strength of concrete are presented in Table 3 for multiple-keyed epoxied joints to compare with Zhou’s experimental results. It can be seen that the absolute difference between numerical and experimental data is at 8.7% on average. It means that the model of multiple-keyed epoxied joint is reliable. The shear strength depends on the concrete property, confining pressure and thickness of epoxy layer. In details, based on the specimens of M1-E1-K3-1 and M1-E1-K3-2 they have the same confining pressure but different concrete compressive strength which is 42.7 and 55.2 MPa respectively, the higher concrete strength, the higher ultimate load of the joint is obtained. Moreover, with the confining pressure increases from 0.5 to 2.0 MPa in specimens M0.5-E2-K3 and M2-E2-K3, the ultimate load rises from 664 to 858 kN, which indicates that at normal concrete strength the confining pressure makes huge contribution to the ultimate shear strength of the joint. Meantime, the ultimate shear load of specimens M1-E1-K3-1 and M1-E2-K3 are 625 and 609 kN, indicating that the ultimate shear strength of joints with 1mm-thick epoxy layer is greater than that of those with 2 mm-thick epoxy layer.

Load-Displacement Relationship

Fig. 2 depicts the relationship between applied load and vertical displacement at top surface of the male-female joint assembly predicted using both values of tensile strength of concrete. It can be clearly seen that the ultimate load and vertical displacement at the ultimate load significantly increase with increasing tensile strength of concrete. For instance, in the case of specimens "*Key epoxy; 1mm 0.69MPa*" and "*Key epoxy; 1mm 2.07MPa*", the vertical displacements calculated using the general assumption of concrete tensile strength increase by about 26% and 16%, respectively, when they are compared with those obtained using lower value of concrete tensile strength, i.e. from the Eurocode 2 formula. Other examples are M1-E1-K1 and M2-E1-K1; the vertical displacements calculated using the general assumption of concrete tensile strength increase by about 16% and 23%, respectively, when they are compared with those obtained using lower value of tensile strength of concrete per the Eurocode 2 formula.

Figs. 3 and 4 present the numerical results of the applied load versus the vertical displacement. It can be noted that there is an obvious drop in loading at the peak load in all curves obtained from numerical analyses which is associated with the brittle failure accompanied by a sudden split between the two parts, male and female, of the joint. The shear capacity of single-keyed epoxied joints largely depends on the confining pressure and the concrete compressive strength as well. Directly after the brittle failure of the keys, the strength of the joint remains constant that is called residual strength. This is due to friction between cracked concrete surfaces under confining pressure. Fig. 3 indicates that the residual strength of a joint is largely dependent on confining pressure. As confining pressure increases from 1.0 to 3.0 MPa for Zhou's specimens, the residual strength generally increases. M3-E1-K1, M3-E2-K1 and M3-E3-K1 demonstrate the highest residual strength, about 300 kN, due to high confining pressure. It can also be observed that the initial stiffness does not change with the increase of confining pressure while the vertical deformation of the joint at ultimate load increases as confining pressure increases. This is not the case of single-keyed dry joints in which the initial stiffness increases by increasing the confining pressure (Shamass et al. 2015). For those single-keyed epoxied joints tested by Buyukozturk et al. (1990), the same findings are also observed, i.e. both ultimate shear strength and residual strength of keyed epoxied joints increase as confining pressure increases (see Fig. 4). Again, initial stiffness does not change with the increase of confining pressure which is confirmed by the experimental results presented by Buyukozturk et al. (1990). The vertical deformation of the joint at ultimate load increases as confining pressure increases as also confirmed by the experimental results of Buyukozturk et al. (1990).

Crack propagation

- ***For single-keyed joints***

Fig. 5 represents the crack propagation of M2-E2-K1. Five points are presented in the figure to demonstrate joint shear behaviours in different stages at the applied load of 280, 294, 306, 333 and 300 kN, which corresponds to the vertical driving displacement of 0.243, 0.290, 0.310, 0.390 and 0.391 mm, respectively. Moreover, Fig. 6 shows the crack patterns of the specimen "*Keyed epoxy; 2mm 3.45 MPa*" at the applied loads of 86, 92, 113 and 85 kN, which corresponds to the applied displacement of 0.316, 0.346, 0.50 and 0.501 mm, respectively

According to the crack propagation of M2-E2-K1 presented in Fig. 5, the crack initially forms at the bottom corner of the key then propagates along the shear plane as the load level closes to the ultimate load. This is coincidence with observation obtained from experiment reported by Zhou et al. (2005) (see Fig. 7a and Fig. 7b). When an epoxied joint reaches its ultimate shear strength, a crack forms suddenly in a brittle manner along the shear plane from the bottom to the top of the keyed area. Moreover, short cracks appear at the concrete region in the male and female parts adjacent to epoxy. Immediately the whole cracks at the shear plane of the male key and the cracks that form through the concrete behind the epoxy layer interconnect causing the ultimate shearing-off failure. This was observed experimentally as shown in the Fig. 7c.

According to the crack propagation of "*Keyed epoxy; 2mm 3.45MPa*" specimen, the crack initially forms at the top and bottom corner of the key then propagates along the shear plane as the shear load increases, which is coincidence with observation obtained from experiment by Buyukozturk et al. (1990) (see Fig. 8a and Fig. 8b). When the joint reaches the maximum load, a crack forms suddenly in a brittle manner along the shear plane from the top to the bottom of the keyed area, which is similar to that observed by Buyukozturk et al. (1990) (see Fig. 8c) in their experiment. Moreover, short cracks appear through the concrete behind the epoxy layer and join the cracks at the shear plane of the male key causing the ultimate shear-off failure. Comparisons between the crack propagation obtained numerically and experimentally of the above examples show that they are highly similar further indicating that the FE model developed in this study for keyed epoxied joint is reliable.

- ***For multi-keyed epoxied joints***

Fig. 9 represents the crack propagation of M1.5-E1-K3, a three-keyed epoxied joint. Five points are presented in the figure to demonstrate the joint shear behaviours in different stages at the applied load of 650, 680, 720, 747 and 800 kN, which corresponds to the vertical displacement of 0.519, 0.561, 0.612, 0.651 and 0.732 mm, respectively. The crack initially forms at the corner of the first and the last key then propagates along the shear plane as the load is gradually increased approaching the ultimate strength, as shown in Fig. 9 at the points 1, 2 and 3. When the joint reaches its ultimate shear strength, a crack forms suddenly in a brittle manner along the shear plane stretching from the top to the bottom of the keys, as shown at the points 4 and 5.

Check for the numerical assumptions

It is mentioned previously that in this study the epoxy was modelled as linear elastic material. This assumption is justified by the fact that the compressive and tensile strength of the epoxy are much higher than the counterpart of the concrete. Moreover, the epoxy-concrete interface is assumed as perfect bond. This assumption is justified again by the fact that the bond strength between the epoxy and concrete is higher than the concrete tensile strength. These assumptions can be confirmed numerically as elaborated as following. Von-Mises yield criterion, which states that a material yields under multi-axial stresses when its distortional energy reaches a critical value, is used here. The Von-Mises stresses computed from the current numerical analyses are less than the tensile yield strength of the epoxy; therefore, the epoxy material does not yield. Moreover, the debonding stress between the epoxy and the concrete is less than the bond strength of the epoxy. These numerical observations justify further that the numerical assumptions taken in this study are appropriate and reliable.

Parametric study

The mechanical properties of epoxy would be affected by the environment conditions. Experimental investigations showed that the development of the mechanical properties of structural epoxy adhesive, the tensile strength and Young's modulus, depend on the curing temperature and time (Maussa et al. 2012). Moreover, Lau and Buyukozturk (2010) observed that the tensile strength and Young's modulus of epoxy decrease with moisture content. Therefore, it is necessary to study the effect of variation of Young's modulus, the only mechanical parameter for linear elastic materials, of the epoxy on the behaviour of single-keyed epoxied joints in addition to the effect of confining pressure. The following shows the FE results for different values of confining pressures and six different values of Young's modulus of epoxy. Parametric study was carried out on the specimens M1-E2-K1 and "*Key epoxy; 2mm 3.45MPa*" which have the concrete compressive strength equal to 53.5 MPa and 45.6 MPa, respectively, and are assigned different values of confining pressure ranged between 1.0 and 5.5 MPa for specimen M1-E2-K1 and between 0.69 and 5.5 MPa for specimen "*Key epoxy; 2mm 3.45MPa*". The elastic modulus of the epoxy is taken as percentage of the elastic modulus of concrete. Therefore, the elastic modulus values of the epoxy material for the case of M1-E2-K1 are 3%E_c, 6%E_c, 13%E_c, 25%E_c, 50%E_c and 75%E_c. For the case of "*Key epoxy; 2mm 3.45MPa*", the elastic modulus values are 3%E_c, 5.7%E_c, 14%E_c, 25%E_c, 50%E_c and 75%E_c.

Load-displacement relationship

Applied load versus the vertical displacement at the top surface of the keyed specimen is shown in Fig. 10 for "*Key epoxy; 2mm 3.45MPa*" and M1-E2-K1. The Young's modulus used for the epoxy are E_{ep}=4826 MPa (=14%E_c) and E_{ep}=9090 MPa (=25%E_c) for specimens "*Key epoxy; 2mm 3.45MPa*" and M1-E2-K1, respectively. The value of E_{ep}=4826 MPa is the same as the one presented in Table 1. It can be seen that the initial stiffness of the joint does not change as confining pressure increases. On the other hand, the vertical displacement at the ultimate load and shear strength of the joint increase as confining pressure increases.

The load-vertical displacement behaviour for the two single-keyed epoxied joints analysed with six different values of epoxy stiffness (Young's modulus) is shown in Fig. 11. The results are found for the specimens "*Key epoxy; 2mm 3.45MPa*" under the applied confining pressure equals to 3.45 MPa. It can be seen that there is a small difference in the initial stiffness of the joint as the stiffness of the epoxy increases. This is because the dimensions of the epoxy are very small compared to the overall dimensions of the joint. However, the displacement at the peak load increases as the epoxy stiffness increases. For instance, increasing the stiffness of the epoxy from 5.7%E_c to 50%E_c increases the deformation by about 13%. Using 50%E_c instead of 14%E_c as the epoxy's elastic modulus results in only 7% increase in the deformation.

Shear strength of the joints

The shear strength/ultimate load of the single-keyed epoxied joints is obtained from numerical analysis under different values of confining pressure and epoxy stiffness. Fig. 12 indicates that there is a linear relationship between the shear capacity of the epoxied joint and the confining pressure for all values of the epoxy stiffness (i.e. elastic modulus). Moreover, shear strength of the joints with low value of epoxy stiffness is less than that of the joints with high value of epoxy stiffness. This can be clearly shown in Fig. 13. For the case of specimen M1-E2-K1, increasing the epoxy stiffness from 3%E_c to 25%E_c can increase its ultimate shear strength by about 10% to 20% depending on the confining pressure. For the case of specimen "*Key epoxy; 2mm 3.45MPa*", increasing the epoxy stiffness from 3% to 25%E_c can increase the ultimate shear strength of the joint by about 10% to 15% depending on the confining pressure. Moreover, it is interesting to notice that as the epoxy stiffness increases to above 25%E_c, the ultimate shear strength of epoxied joints does not change with the respect to epoxy stiffness, i.e. epoxy stiffness does not affect the ultimate shear strength of epoxied joints when it is greater than 25%E_c.

Evaluation of existing formula for determining shear strength of single-keyed epoxied joints

Despite the wealth of experimental research about single-keyed epoxied joints, to the best of the authors' knowledge, no formula for assessing the shear strength of these joints is found except for some empirical formulas, mainly from curve fitting of experimental results, such as the one proposed by Buyukozturk et al. (1990):

$$\tau = 11.1\sqrt{f_{cm}} + 1.2\sigma_c \qquad (5)$$

where τ is the average shear stress in psi along the shear plane; f_{cm} is the compressive strength of concrete in psi; and σ_c is the confining pressure in psi.

The corresponding equation in SI unit is

$$\tau = 0.922\sqrt{f_{cm}} + 1.2\sigma_c = \tau_1 + \tau_2 \quad (6)$$

where τ, f_{cm} and σ_c are all in MPa.

Therefore, the shear strength of the single-keyed epoxied joints

$$V_u = A\,\tau \quad (7)$$

A is the area of the shear plane.

Table 4 contains experimental results (V_{exp}) obtained by Zhou et al. (2005), Buyukozturk et al. (1990), Koseki and Breen (1983) and Mohsen and Hiba (2007) from single-keyed epoxied joints. They are compared with the shear strength values calculated using the empirical equation Eqs. 6 and 7. It can be noted that the proposed empirical formula generally provides higher shear capacity for most of specimens tested by Zhou et al. (2005), Koseki and Breen (1983) and Mohsen and Hiba (2007). On the other hand, the formula provides results which are in very good agreement with the test results by Buyukozturk et al. (1990), which is not surprising as Eq. 6 was derived via curve fitting from the experimental results of Buyukozturk et al. (1990).

As investigated numerically and presented earlier in this paper that in the case of Zhou et al. (2005) specimens, the numerical results agree better with experimental ones when the Eurocode 2 formula is taken to calculate the tensile strength of concrete, while in the case of Buyukozturt et al. (1990) the numerical results are in very good agreement with experimental results when the tensile strength of concrete is taken as 10%f_{cm}. As a result, the chosen concrete tensile strength has significant effect on the calculated shear strength of epoxied joints. Therefore, the proposed empirical formula would provide better results if the tensile strength of concrete is taken the value of 10%f_{cm}, as in the case of Buyukozturk et al. (1990) tests. This may explain why the formula (Eqs. 6 and 7) overestimates the shear capacity of keyed joints tested by Zhou et al. (2005), Koseki and Breen (1983) and Mohsen and Hiba (2007). It would appear to be more reasonable by adapting the empirical formula (Eqs. 6 and 7) as a function of concrete tensile strength f_t.

As can be noticed the second term of the right hand side of Eq. 6 (τ_2) is independent on concrete strength and only depends on the applied confining pressure. Therefore, only the first term of Eq. 6 (τ_1) has to be re-written. Fig. 14 shows the relationship between shear strength of the single-keyed epoxied joint, with a 2 mm-thick epoxy layer, and tensile strength of concrete for Buyutkozturk et at. (1990), and Zhou et al. (2005) specimens at zero confining pressure and f_{cm}=45.9 MPa. It can be clearly noticed that there is a linear relationship between shear stress and tensile strength of concrete. This allows the first term of Eq. 6 to be re-produced using the cross-multiplication with a single variable f_t as shown in Eq. 8.

$$\mathrm{f_t} = 0.1\mathrm{f_{cm}} \rightarrow \tau_1 = 0.922\sqrt{\mathrm{f_{cm}}}$$

$$\text{Any } \mathrm{f_t} \rightarrow \tau_1 = \frac{\mathrm{f_t} * 0.922\sqrt{\mathrm{f_{cm}}}}{0.1\mathrm{f_{cm}}}$$

Therefore,

$$\tau = \tau_1 + \tau_2 = 9.22\,\frac{f_t}{\sqrt{f_{cm}}} + 1.2\sigma_c \tag{8}$$

$$V_u = A\,\tau$$

Table 5 contains the experimental and calculated shear strength results of joints tested by Zhou et al. (2005), Koseki and Breen (1983) and Mohsen and Hiba (2007) adapting the concrete tensile strength from the Eurocode 2 formula. Table 6 shows the experimental and calculated shear strength results of joints tested by Buyukozturk et al. (1990) using the general assumption of concrete tensile strength $\mathrm{f_t} = 10\%\mathrm{f_{cm}}$. It can be noticed from Tables 4 and 5 that the Eq. 8 improves the calculated shear strength but still overestimate the shear strength for specimens with 3 mm-thick epoxy layer because the empirical formula does not take in consideration the effect of epoxy thickness. However, in epoxied joints, the epoxy layer in practice usually has a thickness from 0.8 to 1.6 mm (Buyukozturk et al. 1990) and the most appropriate epoxy thickness in practice is from 1 to 2 mm (Zhou et al. 2005).

Conclusions

The present study has been addressed to investigate the behaviour of single-keyed and multi-keyed epoxied joints used in PCSBs on the basis of accurately modelled, validated and conducted FE analyses of epoxied joints under direct shear. In the proposed FE model, concrete is using the concrete damage plasticity model available in ABAQUS. Two values of concrete tensile strength are adapted, the Eurocode 2 formula and the general assumption of tensile strength of concrete. Because of the tensile strength of epoxy and bond strength of the epoxy-concrete interface are much higher than the tensile strength of concrete, the epoxy is modelled as elastic material and the epoxy-concrete interface is modelled as perfect bond. The FE results in the form of ultimate strength of the keyed joints and cracks evolution in the keyed area are compared with their experiment counterpart. The validated numerical model is then employed for parametric studies, focusing on the effects of confining pressure and elastic modulus of epoxy on shear behaviour of keyed epoxied joints. An empirical formula proposed in the literature to predict the shear strength of single-keyed epoxied joints is evaluated and re-produced by comparing its production of ultimate shear strength to published test results.

The findings are:

- The FE results are in good agreement with experimental results, suggesting that the proposed model is accurate and reliable enough to predict the shear behaviour of single-keyed and multi-keyed epoxied joints. Crack evolution history obtained from numerical analysis accords very well with that from experiments for a wide range of specimens from literature. For all cases, the ultimate shear strength results obtained numerically agree with those obtained experimentally with errors vary in the range -16% to 11.6% for the case of single-keyed joints and -12.5% to 7.6% for the case of multi-keyed ones.

- Concrete tensile strength has significant effect on the behaviour of keyed joints. Increasing the tensile strength of concrete from 7.5%f_{cm} (i.e. per the Eurocode 2 formula) to 10%f_{cm} (i.e. the general assumption) can increase the shear capacity of the joints and the displacement at the peak load up to 25%, depending on the strength of concrete and confining pressure. Therefore in practical design, it is recommended to use concrete tensile strength as accurate as possible.
- The initial stiffness of the keyed epoxied joints does not change as the confining pressure increase. However, the vertical displacement at the peak load and ultimate shear strength of the keyed epoxied joint increase as the confining pressure increase. Moreover, a linear relationship is observed between the confining pressure and the shear capacity of single-keyed epoxied joints.
- As the epoxy stiffness increases from 3%E_c to 15%E_c, the shear strength of the single-keyed epoxied joint increases with the increase of Young's modulus of epoxy in a non-linear manner. In practical design, epoxy with higher Young's modulus should be chosen to be used with shear keys with higher concrete strength. Moreover, the variation in elastic modulus of epoxy has no effect on the ultimate shear strength of the epoxied joints when it is greater than 25%E_c. It is recommended to use epoxy with Young's modulus no less than 25% of that of concrete in epoxied keyed joints for precast concrete segmental bridges.

- The proposed empirical formula can accurately predict ultimate shear capacity of the epoxied joints if taking the tensile strength of the used concrete as 10%f_{cm}. Therefore, the formula for calculating ultimate shear strength of epoxied joints is modified to be explicitly dependent on the tensile strength of concrete. The results calculated by the modified formula then agree better with the experimental counterparts.
- It should be noted that the numerical model established in this study can be used to analyse a range of epoxied keyed joints with different key geometries for which further study is needed in order to produce a shear design formula which is able to explicitly take into account the key geometry for epoxied keyed joints in precast concrete segmental bridges.

Acknowledgements

The financial support from the U.K. Engineering and Physical Sciences Research Council (EPSRC) under the grant of EP/I031952/1 is gratefully acknowledged.

Reference

AASHTO (2003). *Guide Specifications for Design and Construction of Segmental Concrete Bridges*, 2nd Ed., AASHTO, Washington, DC, 92 pages.

Alcalde, M., Cifuentes, H., and Medina, F. (2013). “Influence of the number of keys on the shear strength of post-tensioned dry joints.” *Materiales de Construccion*, 63(310), 297-307.

American Concrete Institute (1997). ACI 349-97, Appendix B, Section B.6.5.2.1.

Bakhoum, M. M. (1990). "Shear behaviour and design of joints in precast concrete segmental bridges," (Doctoral dissertation, Massachusetts Institute of Technology).

Buyukozturk, O., Bakhoum, M. M., and Beattie, S. M. (1990). "Shear behaviour of joints in precast concrete segmental bridges." *J. Struct. Eng.*, 116(12), 3380-3401.

British Standards Institution (2004). BS EN 1992-1-1:2004: Eurocode 2: Design of concrete structures. Part 1-1: general rules and rules for buildings, London, UK.

Cornelissen, H. A. W., Hordijk, D. A., and Reinhardt, H. W. (1986). "Experimental determination of crack softening characteristics of normal weight and lightweight concrete." *HERON*, 31 (2), 45-56.

Gorst, N.J.S., Williamson, S.J., Pallett, P.F. and Clark, L.A. (2003). "Friction in temporary works." The University of Birmingham for the Health and Safety Executive UK, Research Report, 71 (http://www.hse.gov.uk/research/rrpdf/rr071.pdf, accessed on May 10, 2016).

Issa, M., and Abdalla, H. (2007). "Structural behaviour of single key joints in precast concrete segmental bridges." *J. Bridge Eng.*, ASCE, 12(3), 315-324.

Jiang, H., Chen, L., Ma, Z., and Feng, W. (2015). "Shear behaviour of dry joints with castellated keys in precast concrete segmental bridges." *J. Bridge Eng.*, ASCE, 20(2), 04014062 1/12.

Kim, T., Kim, Y., Jin, B., and Shin, H. (2007). "Numerical study on the joints between precast post-tensioned segments." *Int. J. Concr. Struct. Mater.,* 19(1E), 3-9.

Koseki, K., and Breen, J. E. (1983). "Exploratory study of shear strength of joints for precast segmental bridges." (No. FHWA-TX-84-32+ 248-1 Intrm Rpt.). Computer Microfilm International.

Kmiecik, P., and Kaminski, M. (2011). “Modelling of reinforced concrete structures and composite structures with concrete strength degradation taken into consideration.” *Arch*. Civ. Mech. Eng., 11(3), 623-636.

Lau, D., and Buyukozturk, O. (2010). “Fracture characterization of concrete/epoxy interface affected by moisture.” *Mech. Mater.*, 42(12), 1031-1042.

Lubliner, J., Oliver, J., Oller, S., and Onate, E. (1989). “A plastic-damage model for concrete.” *Int. J. Solids Struct.*, 25(3), 299-326.

Mays, G. C., and Hutchinson, A. R. (2005). “Adhesives in civil engineering.” Cambridge University Press.

Moussa, O., Vassilopoulos, A. P., de Castro, J., and Keller, T. (2012). “Early-age tensile properties of structural epoxy adhesives subjected to low-temperature curing.” *Int. J. Adhes. Adhes.*, 35, 9-16.

Qureshi, J., Lam, D., and Ye, J. (2011). “Effect of shear connector spacing and layout on the shear connector capacity in composite beams.” *J. Constr. Steel Res.*, 67(4), 706-719.

Rombach, G. (1997). “Segmental box girder bridges with external prestressing.” *Conference. Actual Problems in Civil Engineering*, St. Petersburg.

Shamass, R., Zhou, X., and Alfano, G. (2015). “Finite-element analysis of shear-off failure of keyed dry joints in precast concrete segmental bridges.” *J. Bridge Eng*., ASCE, 20(6), 04014084-1/12.

Simulia (2011). *ABAQUS Theory Manual*. Version 6.11-1.Dassault Systems.

Turmo, J., Ramos, G., and Aparicio, A.C. (2006). “Shear strength of dry joints of concrete panels with and without steel fibres: Application to precast segmental bridges.” *Eng. Struct.*, 28(1),23-33.

Zhou, X., Mickleborough, N., and Li Z. (2005). “Shear strength of joints in precast concrete segmental bridges.” *ACI Struct. J.*, 102(1), 3-11.

Zhou, X., Mickleborough, N., and Li Z. (2003). “Shear strength of joints in precast concrete segmental bridges.” *Proc., International Conference on Advances in Concrete and Structures,* ICACS, Xuzhou, China, V.2, 1278-1286.

Appendix I Tables

Table 1. Material properties of the epoxy

Young modulus (MPa)	4826
48 hr. compressive strength (MPa)	83
Compressive shear strength/bond strength (MPa)	22
Poisson ratio	0.2

Table 2. Ultimate shear strength of single-keyed epoxied joints: numerical versus experimental ($\mathrm{Error}\ (\%) = \frac{\text{numerical value} - \text{experimental value}}{\text{experimntal value}} * 100$)

Specimen	f_{cm}(MPa)	Experimental Ultimate Strength (kN)	Adapting the concrete tensile strength per Eurocode 2 formula		Adapting the general assumption of concrete tensile strength	
			Numerical Ultimate Strength (kN)	Error (%)	Numerical Ultimate Strength (kN)	Error (%)
M1-E1-K1	53.1	273	288	5.5	344	26.0
M2-E1-K1	53.1	405	357	-11.9	414	2.2
M3-E1-K1	57.6	474	412	-13.1	490	3.4
M1-E2-K1	53.5	251	280	11.6	334	33.1
M2-E2-K1	53.5	377	333	-11.7	403	7.0
M3-E2-K1	55.2	488	408	-16.4	464	-4.9
M1-E3-K1	56.6	265	279	5.3	334	26.0
M2-E3-K1	59.6	318	336	5.7	415	30.5
M3-E3-K1	56.2	355	378	6.5	456	28.5
Key epoxy; 1mm 0.69MPa	44.9	78	69	-11.5	84	7.7
Key epoxy; 1mm 2.07MPa	45.9	101	90	-10.9	102	1.0
Key epoxy; 1mm 3.45MPa	45.6	121	106	-12.4	116	-4.1
Key epoxy; 2mm 3.45MPa	45.6	121	103	-14.9	113	-6.6
Key epoxy; 3mm 3.45MPa	45.6	121	103	-14.9	113	-6.6

Table 3: Ultimate shear strength of multi-keyed epoxied joints: numerical versus experimental

Specimen	f_{cm}(MPa)	Experimental Ultimate Strength (kN)	Numerical Ultimate Strength (kN)	Error (%)
M1-E1-K3-1	42.7	712	625	-12.2
M1-E1-K3-2	55.2	776	764	-1.5
M1.5-E1-K3	52.8	914	800	-12.5
M0.5-E2-K3	52.2	617	664	7.6
M1-E2-K3	41.5	658	609	-7.4
M2-E2-K3	53.3	964	858	-11.0

Table 4: Comparison between experimental and calculated ultimate shear strength of epoxied joints using Eqs. 6-7

Specimen	f_{cm}(MPa)	σ_c(MPa)	A (mm^2)	V_{exp} (kN)	V_u (kN)	V_u/V_{exp}
M1-E1-K1	53.1	1	50000	273	396	1.45
M2-E1-K1	53.1	2	50000	405	456	1.13
M3-E1-K1	57.6	3	50000	474	530	1.12
M1-E2-K1	53.5	1	50000	251	397	1.58
M2-E2-K1	53.5	2	50000	377	457	1.21
M3-E2-K1	55.2	3	50000	488	522	1.07
M1-E3-K1	56.6	1	50000	265	407	1.53
M2-E3-K1	59.6	2	50000	318	476	1.50
M3-E3-K1	56.2	3	50000	355	525	1.48
Key epoxy; 1mm 0.69MPa	44.9	0.69	11613	78	81	1.04
Key epoxy; 1mm 2.07MPa	45.9	2.07	11613	101	101	1.00
Key epoxy; 1mm 3.45MPa	45.6	3.45	11613	121	120	0.99
Key epoxy; 2mm 3.45MPa	45.6	3.45	11613	121	120	0.99
Key epoxy; 3mm 3.45MPa	45.6	3.45	11613	121	120	0.99
Koseki and Breen (1983).	41	2.88	38710	298	362	1.22
Mohsen and Hiba (2007)	30.9	0	117419	454	602	1.33
Mohsen and Hiba (2007)	48.1	0	117419	538	751	1.4

Table 5: Comparison between experimental and calculated ultimate shear strength of epoxied joints using Eq. 8 (with concrete tensile strength per the Eurocode 2 formula $f_t=0.3\ (f_{cm}-8)^{2/3}$)

Specimen	V_{exp}(kN)	V_u (kN) (Eq.8)	V_u/V_{exp}
M1-E1-K1	273	300	1.10
M2-E1-K1	405	360	0.89
M3-E1-K1	474	426	0.90
M1-E2-K1	251	301	1.20
M2-E2-K1	377	361	0.96
M3-E2-K1	488	423	0.87
M1-E3-K1	265	305	1.15
M2-E3-K1	318	368	1.16
M3-E3-K1	355	424	1.20
Koseki and Breen (1983)	298	306	1.03
Mohsen and Hiba (2007)	454	471	1.04
Mohsen and Hiba (2007)	538	549	1.02

Table 6: Comparison between experimental and calculated ultimate shear strength of epoxied joints using Eq. 8 (with concrete tensile strength per general assumption $f_t=10\%f_{cm}$).

Specimen	V_{exp} (kN)	V_u (kN) (Eq.8)	V_u/V_{exp}
Key epoxy; 1mm 0.69MPa	78	81.36086	1.04
Key epoxy; 1mm 2.07MPa	101	101.3863	1.00
Key epoxy; 1mm 3.45MPa	121	120.3798	0.99
Key epoxy; 2mm 3.45MPa	121	120.3798	0.99
Key epoxy; 3mm 3.45MPa	121	120.3798	0.99

Fig. 1. Finite element mesh, boundary conditions and loadings for: (a) Zhou's single-keyed specimens (b) Buyukozturk's specimens (c) Zhou's multiple-keyed specimens

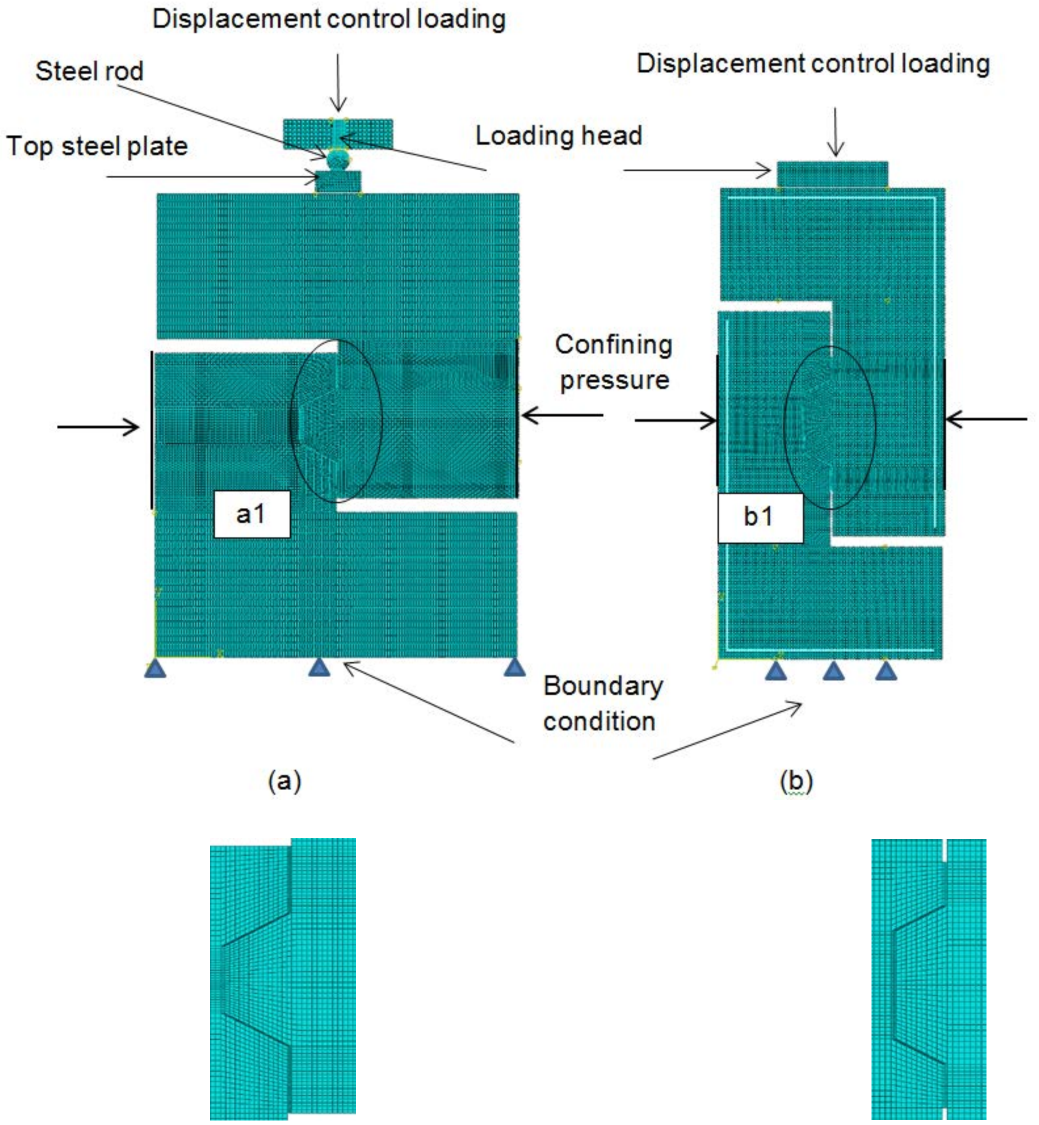

detail a1 detail b1

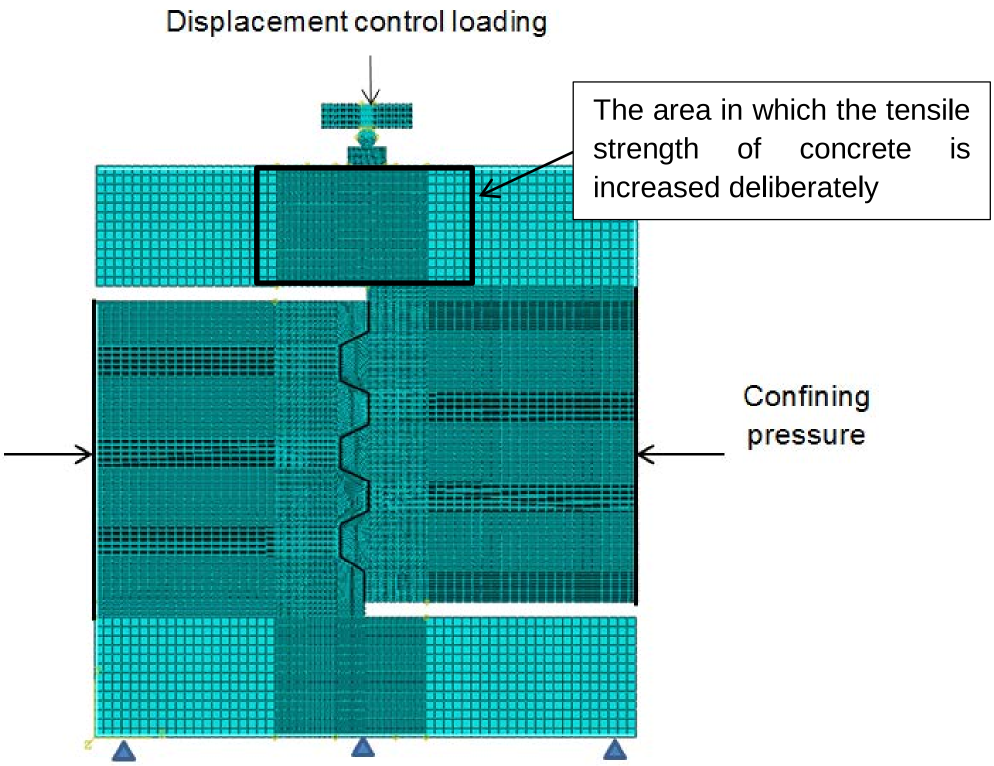
Displacement control loading
The area in which the tensile strength of concrete is increased deliberately
Confining pressure

(c)

Fig. 2. Load-displacement relationships for different specimens using both values of concrete tensile strength

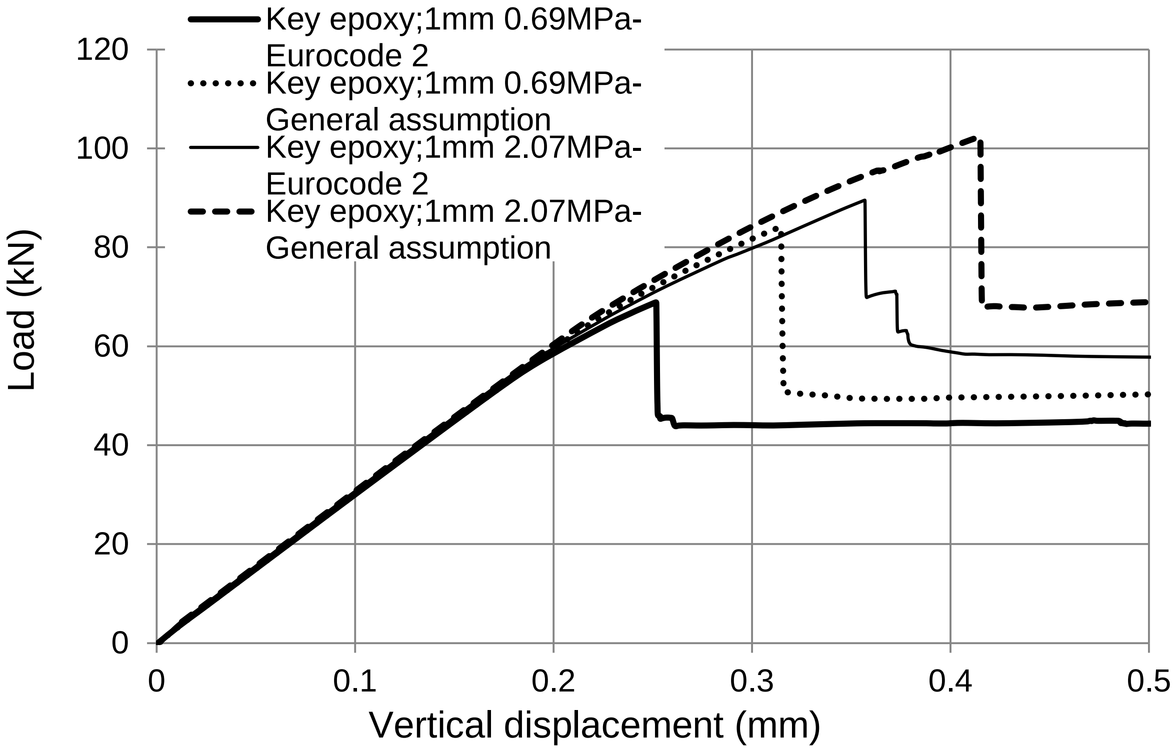

(a)

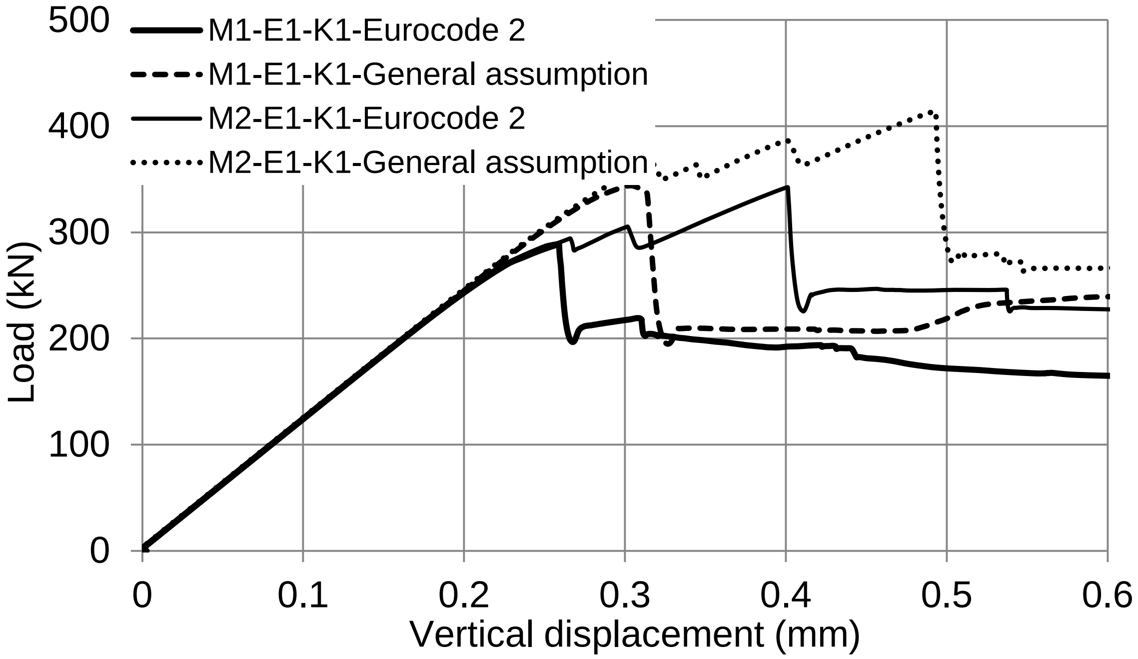

(b)

Fig. 3. Load – displacement relationship from numerical analysis for keyed epoxied joints of Zhou et al. (2005)

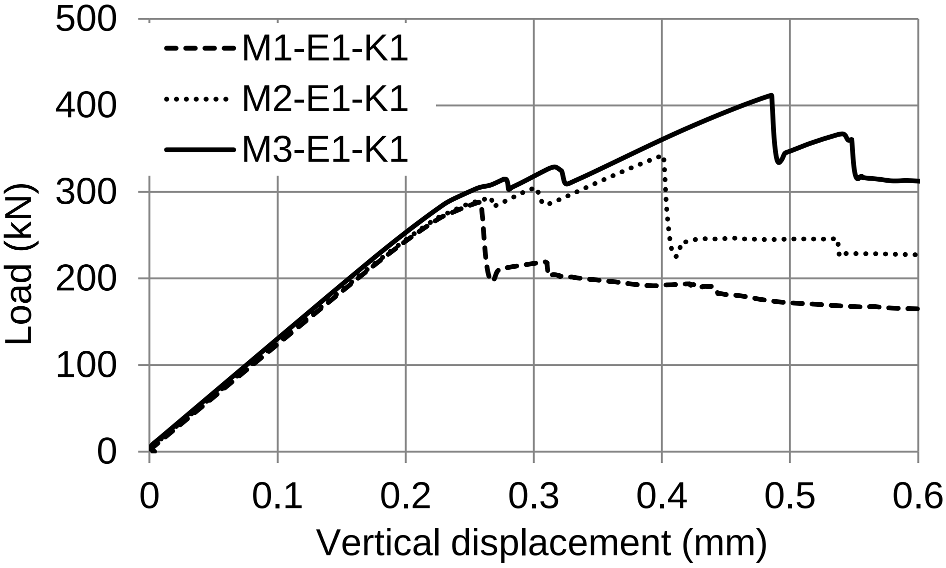

(a)

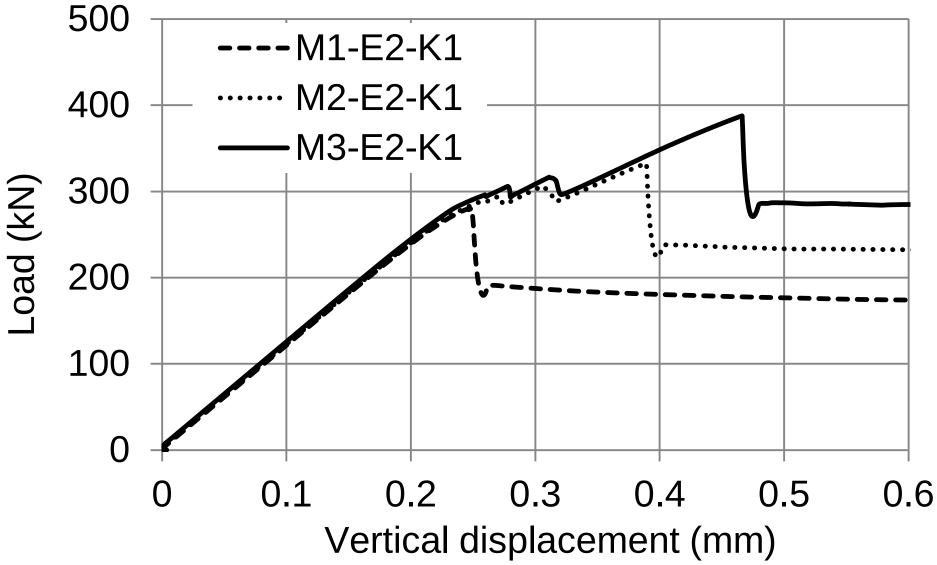

(b)

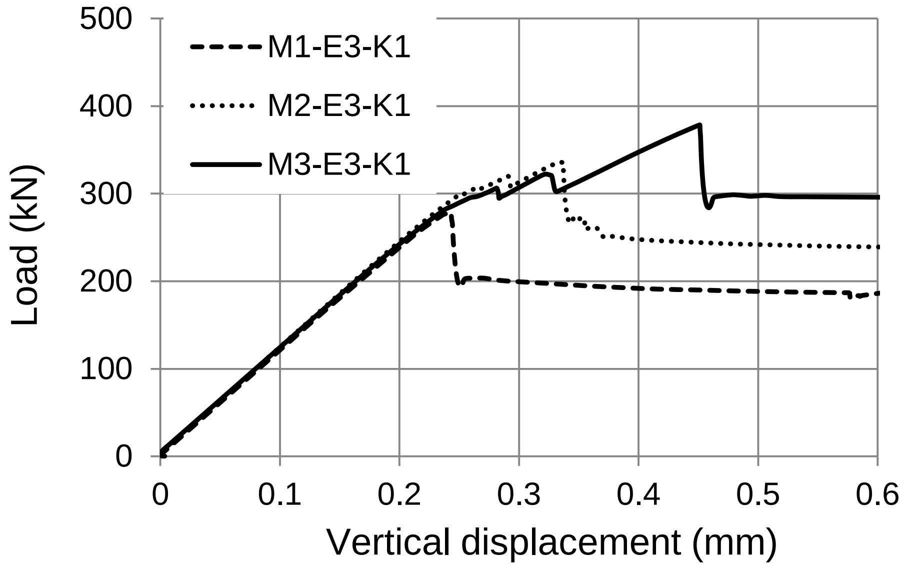
M1-E3-K1
M2-E3-K1
M3-E3-K1
Load (kN)
Vertical displacement (mm)
0
100
200
300
400
500
0
0.1
0.2
0.3
0.4
0.5
0.6

(c)

Fig. 4. Load – displacement relationship from numerical analysis for keyed epoxied joints of Buyukozturk et al. (1990)

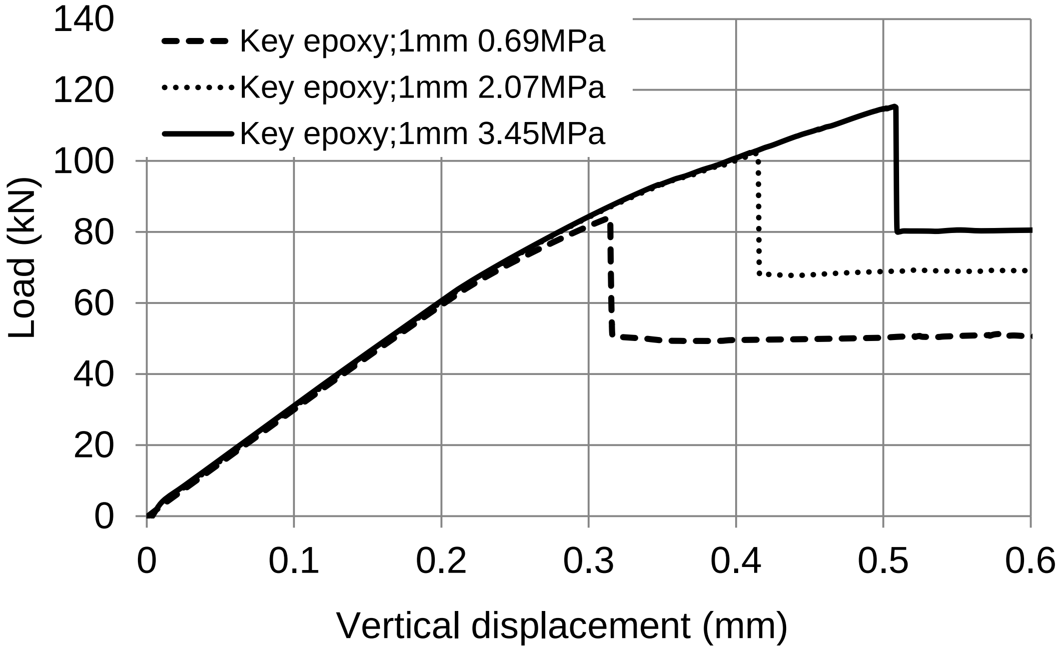

(a)

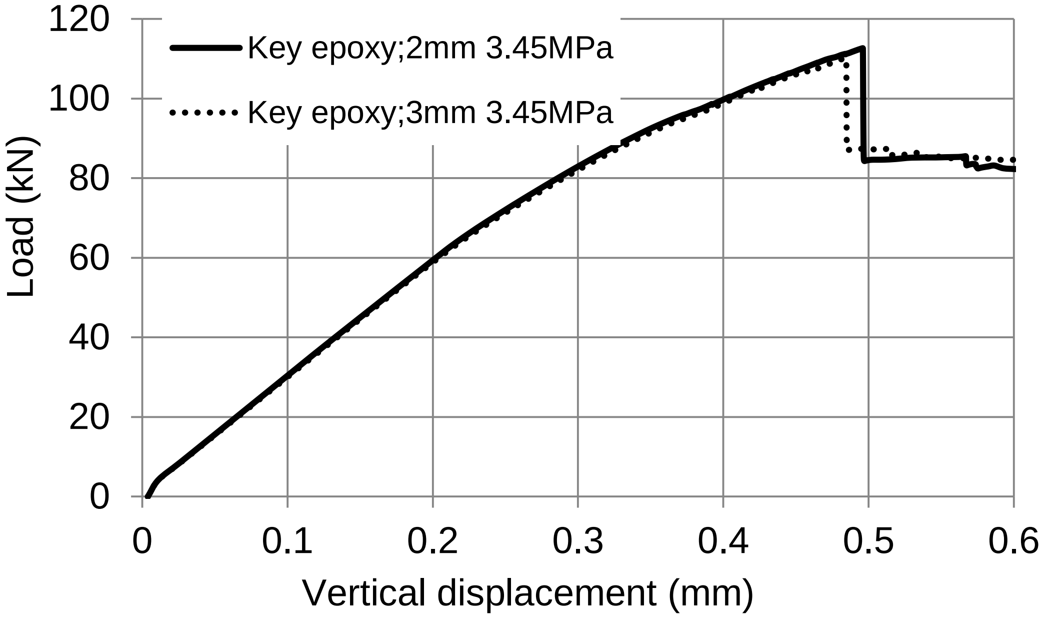

(b)

Fig. 5. Crack patterns of specimens M2-E2-K1 from numerical analyses

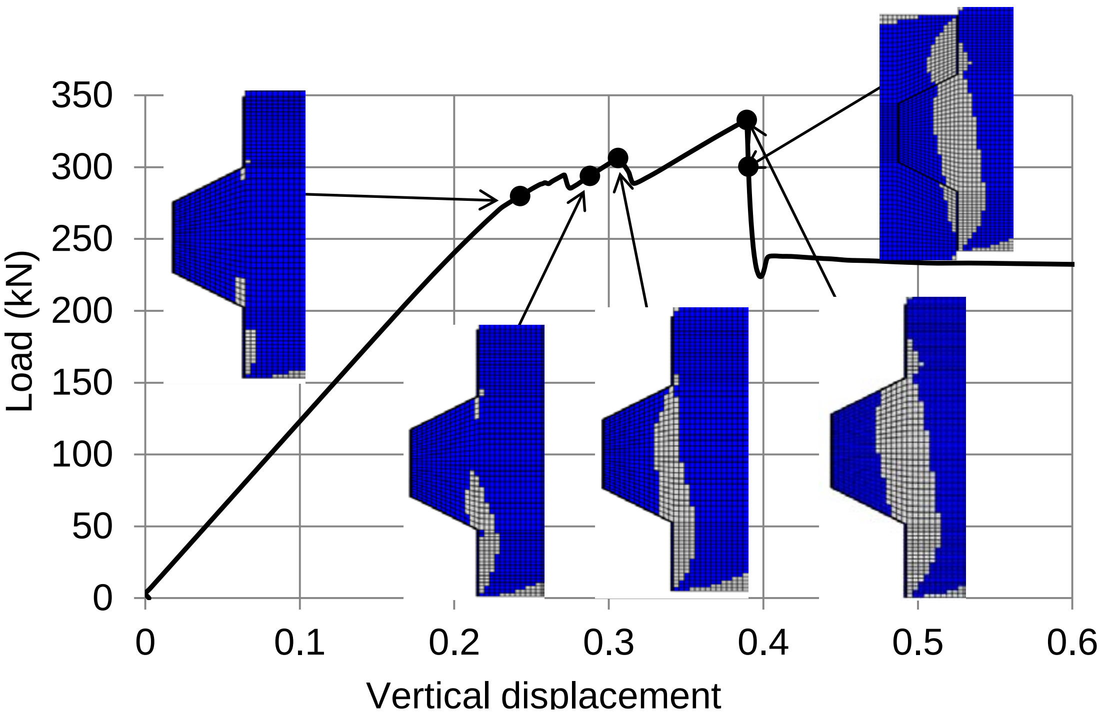

Fig. 6. Crack patterns of specimen “*Keyed epoxy; 2mm 3.45 MPa”* from numerical analyses

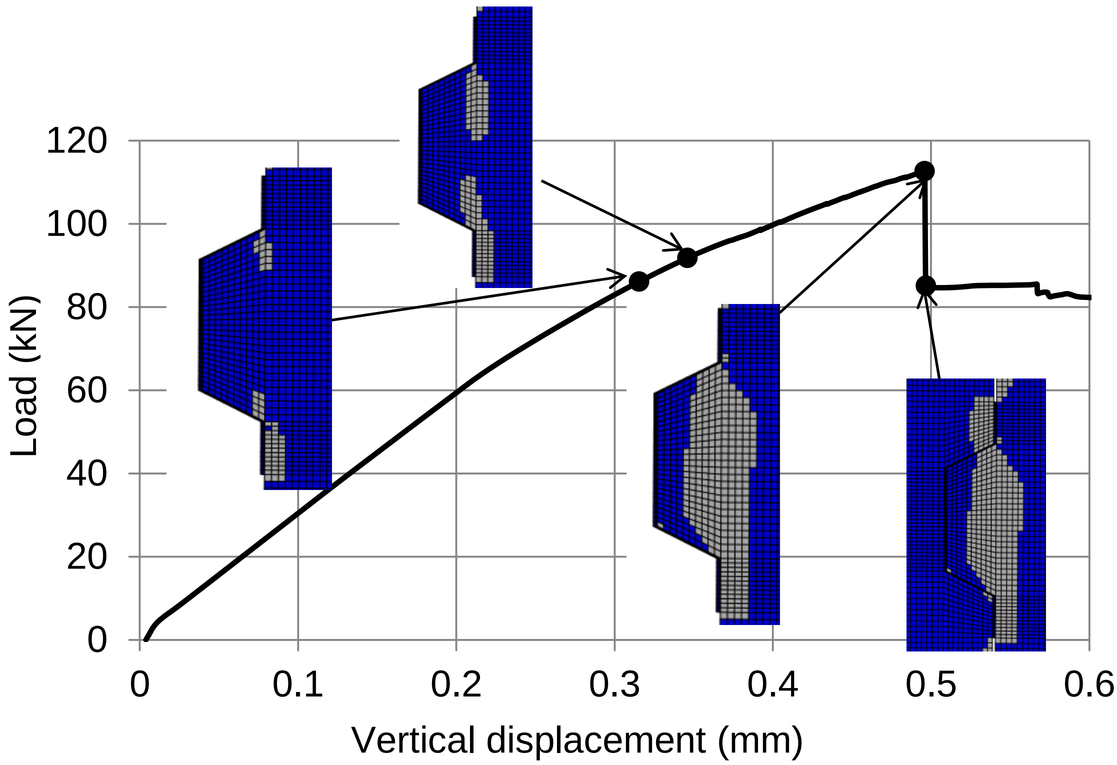

Fig.7. Crack pattern obtained from experiment reported by Zhou et al. (2005) (*reprinted from Zhou et al. (2005) with permission from the American Concrete Institute*)

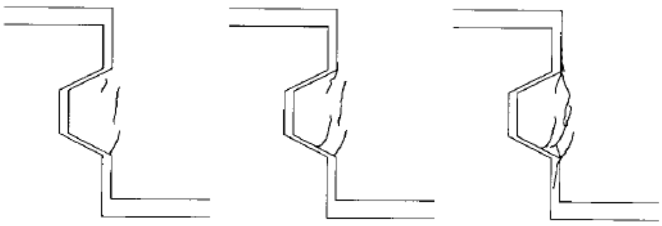

(a) (b) (c)

Fig. 8. Crack pattern obtained from experiment reported by Buyukozturk et al. (1990) (*reprinted from Buyukozturk et al. 1990 with permission from ASCE)*

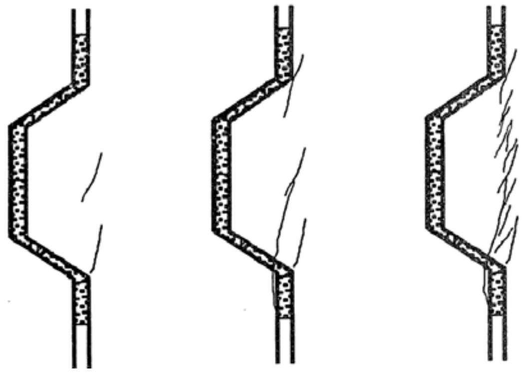

(a) (b) (c)

Fig. 9. Crack propagation of specimen M1.5-E1-K3 from numerical analyses

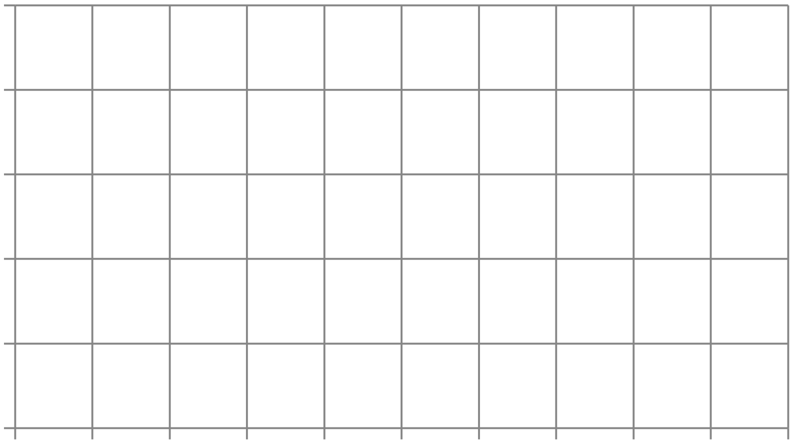

(1) (2) (3) (4) (5)

Fig. 10. Load – displacement curves from numerical analyses for specimens (a) "*Key epoxy; 2mm 3.45MPa*" and (b) M1-E2-K1 under various values of confining pressure

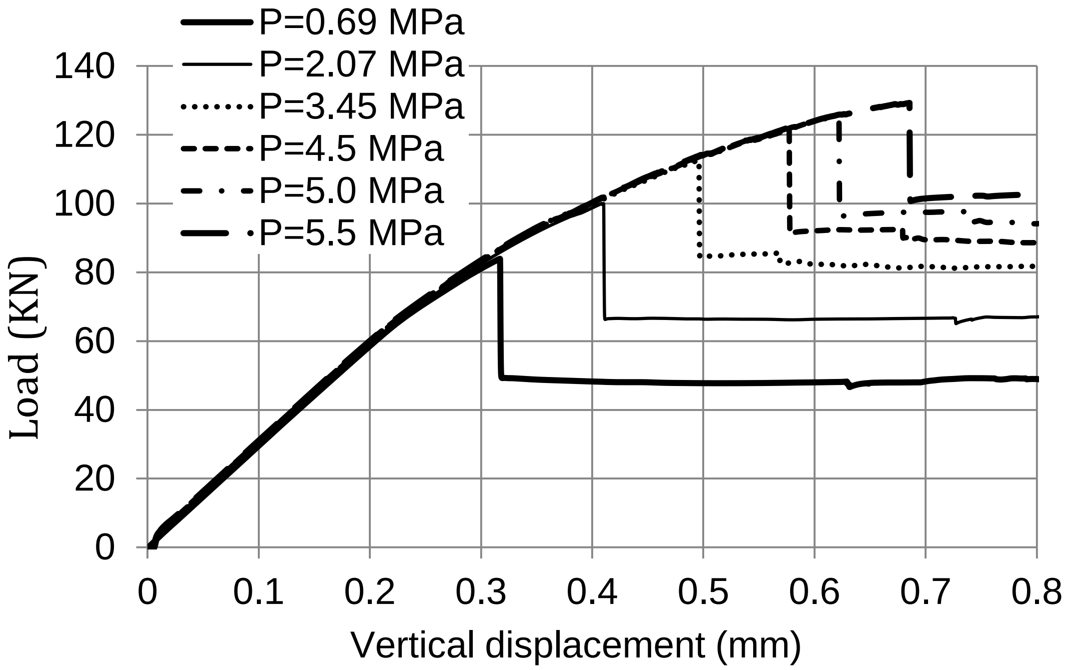

(a)

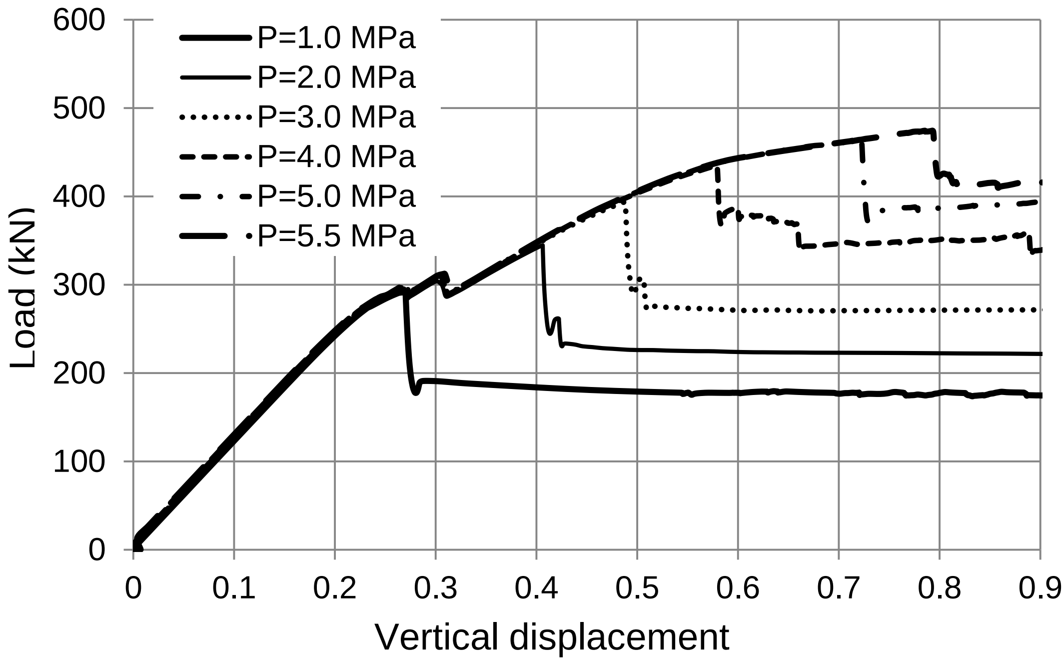

(b)

Fig. 11. Load-displacement relationships from numerical analyses for specimen “*Key epoxy; 2mm 3.45MPa*” using different values of epoxy stiffness

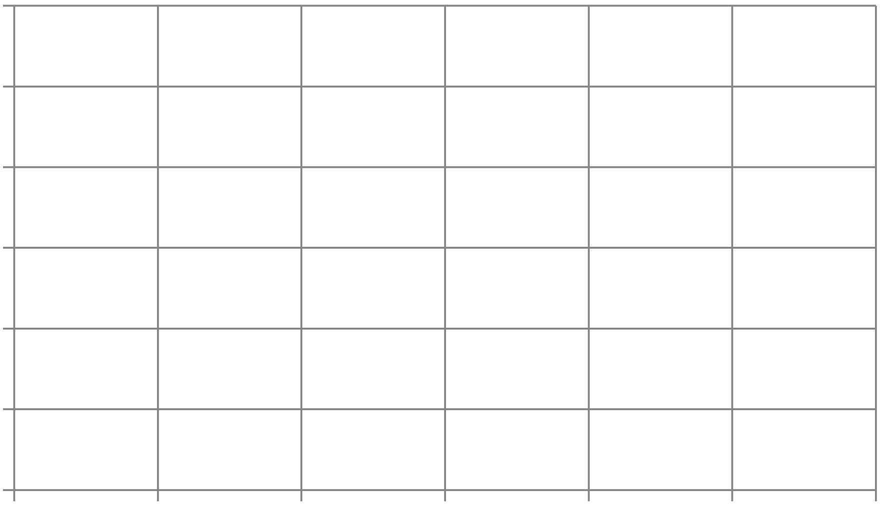

Fig. 12. Ultimate shear capacity versus confining pressure for specimen (a) M1-E2-K1 and (b) "Key epoxy; 2mm 3.45MPa"

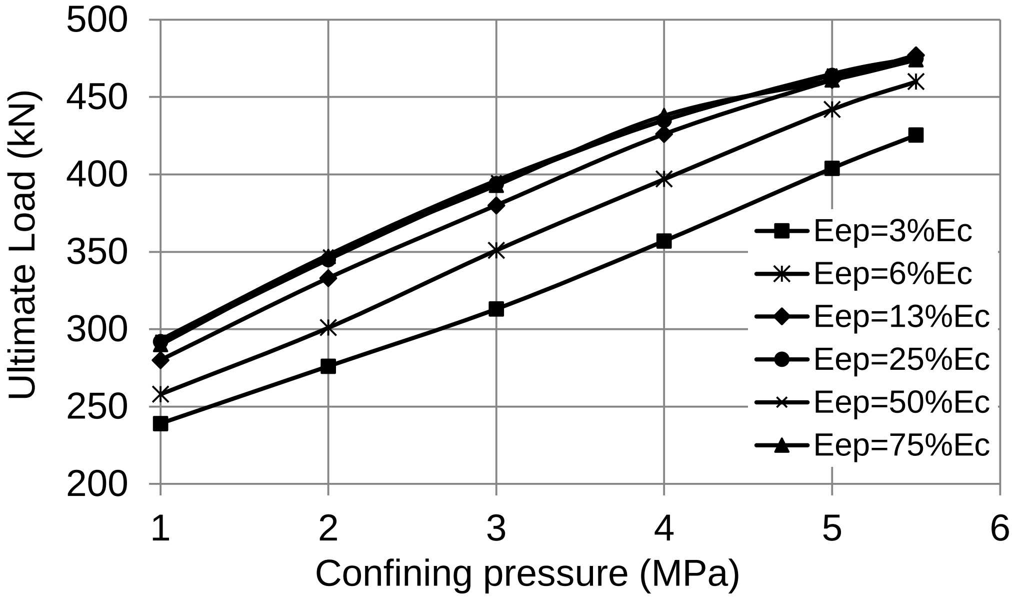

(a)

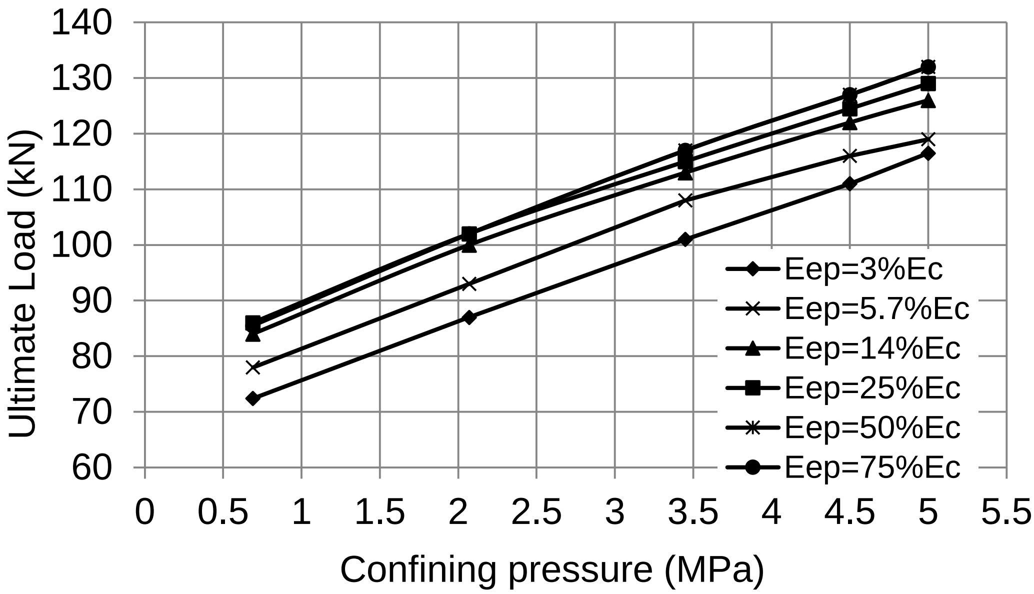

(b)

Fig. 13. Relationship between epoxy stiffness and ultimate shear strength of specimen (a) M1-E2-K1 and (b) “*Key epoxy; 2mm 3.45MPa*” under different values of confining pressure

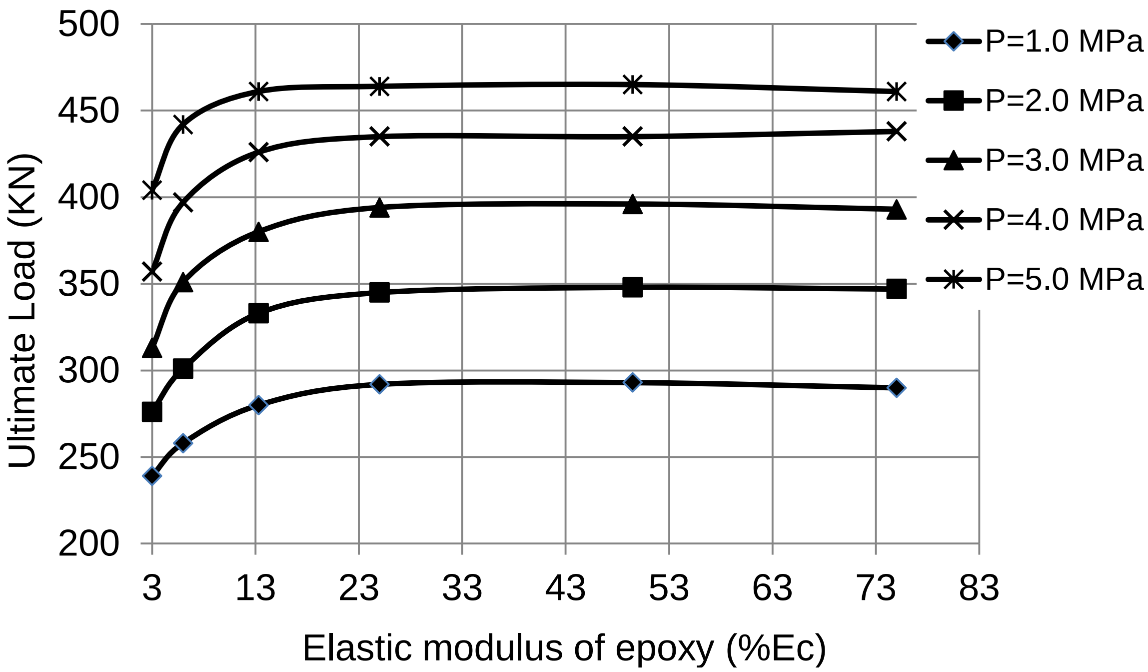

(a)

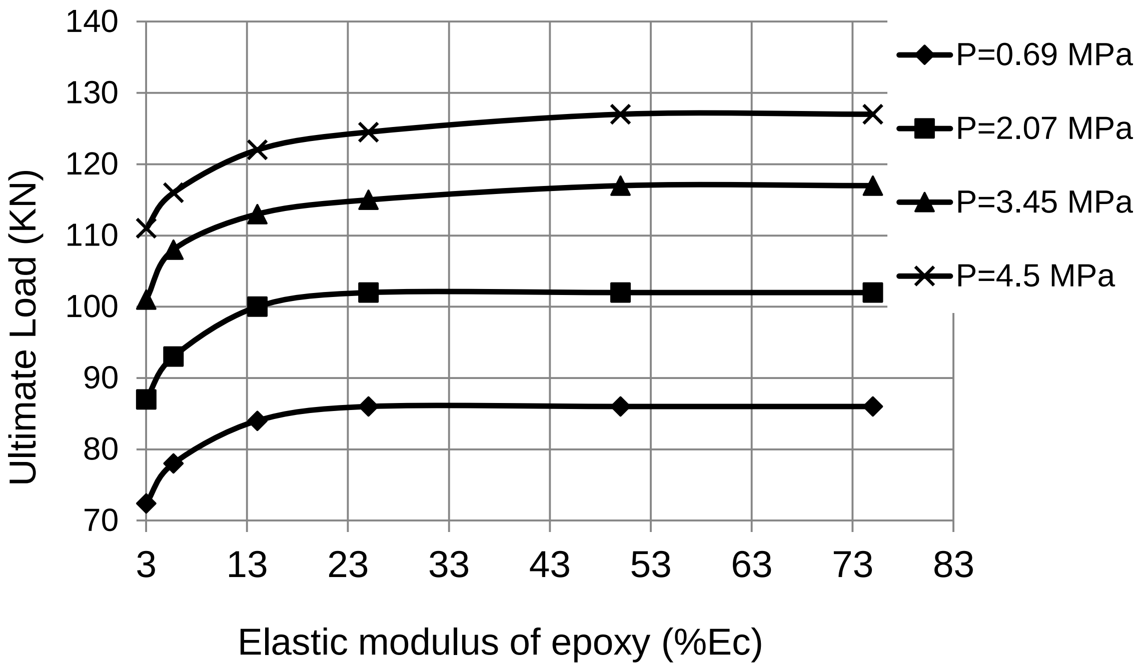

(b)

Fig. 14. Relationship between tensile strength of concrete and ultimate shear stress of the single-keyed epoxied joints